Short communication

Improved protocol for the isolation of naïve follicular dendritic cells

Kazuki Sato[a], Shin-ichiro Honda[a], Akira Shibuya[a, b], Kazuko Shibuya[a, *]

Author information

[a]Department of Immunology, Faculty of Medicine, [b]Life Science Center of Tsukuba Advanced Research Alliance (TARA), University of Tsukuba, 1-1-1, Tennodai, Tsukuba, Ibaraki 305-8575, Japan.

Email addresses

K. Sato: s0710709@gmail.com

K. Shibuya: kazukos@md.tsukuba.ac.jp

S. Honda: shonda@md.tsukuba.ac.jp

A. Shibuya: ashibuya@md.tsukuba.ac.jp

Author contributions: K. Sato, S. Honda, A. Shibuya, and K. Shibuya designed research and analyzed the data. K. Sato, and K. Shibuya performed research. K. Sato, A. Shibuya, and K. Shibuya wrote the paper. All authors read and approved the final manuscript.

The authors declare no conflict of interest.

*Corresponding author. Kazuko Shibuya, MD, PhD

E-mail: kazukos@md.tsukuba.ac.jp

Department of Immunology, Faculty of Medicine, University of Tsukuba, 1-1-1, Tennodai, Tsukuba, Ibaraki 305-8575, Japan; Phone: (+81) 29-853-3281, Fax: (+81) 29-853-3410

Abstract

Follicular dendritic cells (FDCs) in lymphoid organs play an important role in the humoral immune response. However, because the isolation of FDCs is difficult due to their very small population size and fragility under mechanical and chemical stresses, the genetic and biochemical characteristics of FDCs remain unclear. Previously, we identified FDCs as ICAM-1$^+$ cells in the CD45$^-$ non-hematopoietic cell fraction from naïve mouse spleen after cell separation by means of digestion with a combination of enzymes. In the present study, using a new combination of enzymes, we found that FDCs are highly enriched in the CD45$^-$ICAM-1$^+$CD21/35$^+$ cell fraction. CD45$^-$ICAM-1$^+$CD21/35$^+$ cells in the mouse spleen retained an antigen administered *in vivo* for more than 7 days. Moreover, CD45$^-$ICAM-1$^+$CD21/35$^+$ cells isolated from the spleen of mice administered with a cognate antigen enhanced the survival and proliferation of antigen-specific B cells *in vitro*. Our improved protocol for the isolation of naïve FDCs will be useful for the analysis of FDCs *in vitro* and *in vivo*.

Keywords

Follicular dendritic cells; Isolation methods; Stromal cells; Antigen presentation; Antigen retention.

1. Introduction

Follicular dendritic cells (FDCs) were identified in 1965 as antigen-retaining reticular cells in lymphoid organs (Mitchell and Abbot, 1965). FDCs are non-hematopoietic antigen-presenting cells that can be distinguished from conventional dendritic cells (Chen et al., 1978a, 1978b; Turley et al., 2010). FDCs present antigen via CD21/35 to B cells and support the clonal expansion of B cells in germinal center and immunoglobulin class-switching, and for the B-cell-receptor gene to undergo somatic hypermutation (Victora and Nussenzweig, 2012). Thus, FDCs play an important role in the humoral immune response.

Immunohistochemical analysis has partially revealed the phenotypic characteristics of FDCs; however, because the isolation of FDCs is difficult due to their scarcity in lymphoid organs and their fragility under mechanical and chemical stresses, the molecular and functional characteristics of FDCs remain unclear. Conventionally, FDCs are isolated as FDC-M1$^+$ cells by using magnetic cell-separation technology after

whole-body irradiation and enzymatic digestion (Sukumar et al., 2006). However, the molecular marker FDC-M1 is detected not only in FDCs but also in cells located in the marginal sinus and tingible body macrophages (Kranich et al., 2008; Krautler et al., 2012). In addition, whole-body irradiation induces systemic inflammation through the release of damage-associated molecular pattern molecules from damaged tissue (Schaue et al., 2015), which might cause unexpected FDC activation. Thus, FDCs isolated after whole-body irradiation are not suitable for the biological study of naïve FDCs. Although previous reports described FDCs isolated from lymph nodes of naïve mice without irradiation (Fasnacht et al., 2014; Jarjour et al., 2014; Tamburini et al., 2014), phenotypical and functional characteristics of those FDCs were unclear.

Previously, we reported a unique method to isolate FDCs from the CD45^{-}ICAM-1^{+} cell population in the lymphoid organs of non-irradiated naïve mice by means of flow cytometry (Usui et al., 2012). In the present study, we used a new combination of enzymes for cell separation to subdivide

1 the CD45^{-}ICAM-1^{+} cell population into CD21/35^{+} and CD21/35^{-} cell

2 populations. Here we describe this improved method for producing highly

3 enriched preparations of FDCs.

4

2. Materials and methods

2.1. Mice

C57BL/6J mice were purchased from Clea Japan Inc. (Tokyo, Japan) and maintained under specific pathogen-free (SPF) conditions. Quasi-monoclonal (QM) mice, in which transgenic B cell receptor specifically reacts with 4-hydroxy-3-nitrophenylacetyl (NP) antigen, are homozygous for the *Vht* gene (*Vht*/*Vht*, $J\kappa^-/J\kappa^-$, λ^+/λ^+). All experiments were performed according to the guidelines of the Animal Ethics Committee of the University of Tsukuba Animal Research Center.

2.2. Antibodies and reagents

Fluorescein isothiocyanate (FITC)-conjugated anti-mouse CD31 (clone, 390), R-phycoerythrin (PE)-conjugated anti-mouse ICAM-1 (3E2), anti-mouse CD45.2 (104), Alexa647-conjugated anti-mouse CD31 (390), allophycocyanin (APC)-conjugated anti-mouse CD19 (1D3), anti-mouse CD45R/B220

(RA3-6B2), Horizon V450-conjugated anti-mouse CD45.2 (104), and biotin-conjugated anti-mouse CD45 (30-F11) monoclonal antibodies (mAbs) were purchased from BD Biosciences (San Jose, CA, USA). Purified anti-mouse CD16/32 (2.4G2), and PECy7-conjugated rat IgG2a isotype control (2A3) mAbs were purchased from Tonbo Biosciences (San Diego, CA, USA). PECy7-conjugated anti-mouse CD21/35 (7G6), biotin-conjugated anti-mouse CD45R/B220 (RA3-6B2), and biotin-conjugated anti-mouse Ter119 (Ter-119) mAbs were purchased from BioLegend (San Diego, CA, USA). eFluor660-conjugated anti-mouse podoplanin (PDPN) (eBio8.1.1) mAb was purchased from eBioscience (San Diego, CA, USA). Biotin-conjugated anti-FDC-M2 (FDC-M2) mAb was purchased from ImmunoKontact (Abingdon, UK). NP-Ficoll and 2, 4, 6-trinitrophenyl (TNP)-Ficoll were purchased from Biosearch Technologies (Novato, CA, USA) and TNP-Ficoll was labeled to produce FITC-TNP-Ficoll by using a FluoReporter FITC Labeling Kit (Thermo Fisher Scientific, MA, USA), in accordance with the manufacturer's instructions.

2.3. Isolation of stromal cell subsets

Stromal cells were isolated by using a method reported previously with modifications (Usui et al., 2012). Spleen from naïve mice was minced into a homogenous paste with a scalpel on a dish plate and then treated with 2 ml of an enzyme cocktail containing 1 mg/mL collagenase D (Roche, Indianapolis, IN, USA), 100 μg/mL DNase I (Sigma, St. Louis, MO, USA) and 0.6 U/mL Dispase (Roche, Indianapolis, IN, USA) in complete Dulbecco's modified Eagle's medium (cDMEM) containing 2% fetal bovine serum (FBS). After incubation in a 24-well plate for 30 min at 37°C in a humidified incubator, cell suspensions were passed through a 100 μm nylon cell strainer (Corning, NY, USA) and cells were resuspended in cDMEM containing 10% FBS and 5 mM ethylenediaminetetraacetic acid (EDTA). For lysis of red blood cells, cells were incubated with 1 ml of ammonium-chloride-potassium lysing buffer for one spleen for 2 min, washed once with cDMEM, and subsequently once with the washing buffer (PBS containing 2 % FBS and 5

mM EDTA). Cells were resuspended in the washing buffer at 10^9/ml and incubated with 2.5 μg purified anti-mouse CD16/32 mAb for 10^8 cells for 20 min on ice. Cells were then stained with a biotin-conjugated anti-mouse mAbs cocktail containing anti-CD45 (2.5 μg), anti-B220 (1 μg), and anti-anti-Ter119 (1 μg) for 10^8 cells for 30 min on ice. Unlabeled cells were then negatively selected by magnetic separation with BD IMag SAv particles (BD Pharmingen, San Diego, CA) in accordance with the manufacturer's instructions. Finally, cells were stained with V450-conjugated anti-CD45.2, FITC or Alexa647-conjugated anti-CD31, eFlour660-conjugated anti-PDPN, PE-conjugated anti-ICAM-1, and PECy7-conjugated anti-CD21/35 mAbs for 30 min on ice, washed with the washing buffer, passed through a 100 μm-nylon cell strainer, and analyzed by flow cytometry (FACSAria, BD Biosciences). Doublet and dead cells were gated out on the basis of forward-scatter A (FSC) and FSC H properties and PI staining, respectively. $CD45^-ICAM\text{-}1^+CD21/35^+$ cells and other stromal cells were sorted by using a flow cytometry (FACSAria) (100 μm-nozzle; 20 psi). For evaluation of B cell

contamination in CD45$^-$ICAM-1$^+$CD21/35$^+$ fraction, anti-B220 mAb was excluded from antibody mixture for negative selection of lineage cells. For the analyses of the FDC-M2 expression on CD45$^-$ICAM-1$^+$CD21/35$^+$ cells, the stromal cells were enriched with BD IMag PE particles (BD Pharmingen, San Diego, CA), instead of BD IMag SAv particles, after staining with PE-conjugated anti-mouse CD45.2 mAb.

2.4. Antigen retention analysis

C57BL/6J mice were immunized intravenously with 50 μg FITC-TNP-Ficoll or phosphate-buffered saline as control. Seven days later, retention of the FITC-conjugated antigen by stromal cell subsets was analyzed by means of flow cytometry.

2.5. Ex vivo antigen presentation to cognate B cells

Naïve QM and WT B cells were purified from naïve mouse spleen by using anti-B220 particles-DM (BD Pharmingen), in accordance with the

manufacturer's instructions, and then labeled with 500 nM carboxyfluorescein diacetate succinimidyl ester (CFSE). To assess B-cell proliferation, CFSE-labeled B cells (5×10^3 cells) were co-cultured in cDMEM medium containing 10% FBS in 96-well round-bottom plates with purified $CD45^-ICAM\text{-}1^+$ cells (500 cells) or $CD45^-ICAM\text{-}1^+CD21/35^+$ cells (500 cells) cells isolated from mice given 50 μg NP-Ficoll intravenously seven days previously. Three days later, the cells were harvested and stained with APC-conjugated anti-CD19 monoclonal antibodies. The ratio of PI^- cells in the $CD19^+$ gate was used as an index of B-cell survival. The proliferation of PI^-CD19^+ cells was analyzed by means of the CFSE dilution assay.

2.6. Quantitative polymerase chain reaction

Total RNA was isolated by using Isogen reagent (Nippon Gene, Tokyo, Japan). For reverse transcription, we used a high-capacity complementary DNA reverse-transcription kit (Applied Biosystems, Carlsbad, CA, USA). Real-time polymerase chain reaction (PCR) analysis of *Mfge8*, *Cxcl13*,

Fcgr2b, *Cr2*, *Icam1*, *Vcam1*, *Fcamr*, *Stab2*, *Ccl19*, and *Pdgfrb* was performed by using an ABI 7500 sequence detector (Applied Biosystems), Power SYBR Green PCR master mix (Applied Biosystems), and the appropriate primers. The *Actb* expression level was measured as the internal control to normalize the data. The primer sequences for the target genes were as follows: *Mfge8*: forward, 5'-ATA TGG GTT TCA TGG GCT TG-3', reverse, 5'-GAG GCT GTA AGC CAC CTT GA-3'; *Cxcl13*: forward, 5'-CAT AGA TCG GAT TCA AGT TAC GCC-3', reverse, 5'-TCT TGG TCC AGA TCA CAA CTT CA-3'; *Fcgr2b*: forward, 5'-TGC TGT CGC AGC CAT TGT TA-3', reverse, 5'-TGT TGG CTC CAG TCC AGA TG-3'; *Cr2*: forward, 5'-AAT TGC AAA TGG TGG TCA CA-3', reverse, 5'-GAT CGG GGC AAT GAG TTA GA-3'; *Icam1*: forward, 5'-TTG AGA ACT GTG GCA CCG TG-3', reverse, 5'-CAG CTC CAC ACT CTC CGG AA-3'; *Vcam1*: forward, 5'-GTG ACC TGT CTG CAA AGG AC-3', reverse, 5'-AAA GGG ATA CAC ATT AGG GAC TG-3'; *Fcamr*: forward, 5'-CCC AGC CTG AGA ACG AGA TG-3', reverse, 5'-AGA GAT GGG TCC TGA ACT GAG-3'; *Stab2*: forward, 5'-TCA AGA CGG AGT GCC AGT C-3', reverse,

5'-GCA ATC TCG AAC CCC GAC A-3'; *Ccl19*: forward, 5'-TTC ACG CCA CAG GAG GAC ATC T-3', reverse, 5'-CCA CAC TCA CAT CGA CTC TCT AGG C-3'; *Pdgfrb*: forward, 5'-TCA AGC TGC AGG TCA ATG TC-3', reverse, 5'-CCA TTG GCA GGG TGA CTC-3'; *Actb*: forward, 5'-ACT GTC GAG TCG CGT CCA-3', reverse, 5'-GCA GCG ATA TCG TCA TCC AT-3'. The thermal cycling conditions comprised an initial denaturation step at 95˚C for 10 min, followed by 40 cycles at 95˚C for 15 s and 60˚C for 1 min. The mRNA level was determined relative to that in $CD45^{-}ICAM\text{-}1^{+}$ cells.

2.5. Statistical analysis

Statistical analysis was performed by using the ANOVA followed by the post-hoc Tukey-Kramer test in the GraphPad Prism 5 software (GraphPad Software, Inc., San Diego, CA, USA).

3. Results and Discussion

3.1. Isolation of CD45$^-$ICAM-1$^+$CD21/35$^+$ cells from the spleen of naïve mice

We found that by using an improved combination of enzymes for cell separation the CD45$^-$ICAM-1$^+$ cell population could be further divided into populations of CD21/35$^+$ and CD21/35$^-$ cells (Fig. 1A). In our previous report, we used a high concentration of collagenase D (33.3 mg/mL) (Usui et al., 2012); however, this caused downregulation of CD21/35 expression on the cell surface (Supplementary Fig 1). In the present study, we found that digestion with a low concentration of collagenase D (1 mg/mL) did not affect CD21/35 expression (Supplementary Fig 1) and that the addition of dispase increased the yield of CD45$^-$ICAM-1$^+$CD21/35$^+$ cells (Table 1).

Flow cytometric analysis showed that CD45$^-$ICAM-1$^+$CD21/35$^+$ cells did not express the cell markers CD31 or PDPN, suggesting that blood endothelial cells (BECs, CD45$^-$ICAM-1$^+$CD31$^+$) and fibroblastic reticular cells (FRCs, CD45$^-$ICAM-1$^+$PDPN$^+$) were not contaminated in the CD45$^-$ICAM-1$^+$CD21/35$^+$ cell fraction (Fig. 1A). In contrast to a previous

report describing that $CD35^+$ FDCs can be divided into $PDPN^+$ or $PDPN^-$ population in lymph nodes (Link et al., 2007), we found that splenic $CD45^-$ICAM-$1^+CD21/35^+$ cells isolated with our method did not express PDPN (Fig. 1A). Previous reports have suggested that the developmental mechanisms of FDCs are different between lymph nodes and spleen (Castagnaro et al., 2013; Jarjour et al., 2014; Krautler et al., 2012); therefore, FDCs might show some different phenotypes between the lymph nodes and spleen. We also confirmed that $CD45^-$ICAM-$1^+CD21/35^+$ cells did not contain $B220^+$ cells, indicating that B cells were not contaminated in this fraction (Fig. 1B). Taken together, these data suggest that the isolated $CD45^-$ICAM-$1^+CD21/35^+$ cells are highly enriched FDCs.

FDC-M2 is an well known FDC marker in immunohistochemical analysis. Indeed, flow cytometric analysis showed that most $CD45^-$ ICAM-$1^+CD21/35^+$ cells expressed FDC-M2 (Fig. 1C). However, FDC-M2 was also significantly detected on $CD45^-$ICAM-1^+CD31^+ BECs, which is over 95 % population in the $CD45^-$ICAM-1^+ fraction (Fig. 1C), indicating that the

major FDC-M2$^+$ population is BECs rather than FDCs.

3.2. FDC marker gene expression in CD45$^-$ICAM-1$^+$CD21/35$^+$ cells

Immunohistochemical analysis has revealed that within the stromal cell fraction FDCs are characterized by the expression FDC-M1 (*Mfge8*), FcγRIIB (*Fcgr2b*), CXCL13 (*Cxcl13*), CD21/35 (*Cr2*), ICAM-1 (*Icam1*), VCAM-1 (*Vcam1*), and Fcα/μR (*Fcamr*) (Allen and Cyster, 2008; Honda et al., 2009). To examine whether FDC purity was increased in the CD45$^-$ICAM-1$^+$CD21/35$^+$ cell fraction compared with that in the CD45$^-$ICAM-1$^+$ cell fraction, the expression of phenotypic markers was examined. We found that CD45$^-$ICAM-1$^+$CD21/35$^+$ cells expressed significantly greater levels of FDC-related genes ($P < 0.001$) compared with CD45$^-$ICAM-1$^+$ cells and two other stromal cell subsets (i.e., BECs and FRCs), indicating that the number of FDCs in the CD45$^-$ICAM-1$^+$CD21/35$^+$ cell fraction was significantly higher than in the CD45$^-$ICAM-1$^+$ cell fraction (Fig. 1D). Moreover, CD45$^-$ICAM-1$^+$CD21/35$^+$ cells showed a significantly

lower expression of *Stabilin2*, *Ccl19*, and *Pdgfrb*, which are markers of BECs, FRCs, and splenic immature FDCs, respectively (Fig. 1E) (Krautler et al., 2012; Link et al., 2007; Sørensen et al., 2012), indicating that the CD45$^-$ICAM-1$^+$CD21/35$^+$ cell population was highly enriched with FDCs isolated from the spleen of naïve mice.

3.3. Antigen retention by CD45$^-$ICAM-1$^+$CD21/35$^+$ cells in vivo

FDCs are capable of retaining opsonized antigen, which is required for germinal center maintenance and the establishment of long-term immune memory (Mandel et al., 1980; Victora and Nussenzweig, 2012). Therefore, we next examined the antigen retention of CD45$^-$ICAM-1$^+$CD21/35$^+$ cells. Because FDCs retain intact antigen not only on the cell surface but also within recycling endosomal compartments for long-term storage (Heesters et al., 2013), mice were given FITC-labeled antigen to allow detection of the antigen on cell surfaces and in the cytosol of the stromal cells. Although the fluorescence signal was not detected in

CD45⁻ICAM-1⁺ cells, BECs, or FRCs 7 days after antigen administration, a significant increase ($P < 0.01$) in fluorescence intensity was detected in CD45⁻ICAM-1⁺CD21/35⁺ cells isolated from mice administered the FITC-labeled antigen (Fig. 2A, B), indicating that CD45⁻ICAM-1⁺CD21/35⁺ cells retained the antigen for at least 7 days. Because FDCs are the only cells that retain intact antigens for long periods of time (Mandel et al., 1980), our study showed that the isolated CD45⁻ICAM-1⁺CD21/35⁺ cells exhibited not only the phenotypical but also the functional features of FDCs.

3.4. Antigen presentation to cognate B cells by CD45⁻ICAM-1⁺CD21/35⁺ cells

To investigate whether CD45⁻ICAM-1⁺CD21/35⁺ cells initiate the proliferation of cognate B cells, we isolated CD45⁻ICAM-1⁺ cells and CD45⁻ICAM-1⁺CD21/35⁺ cells from mice administered with NP-Ficoll and co-cultured the cells with CFSE-labeled QM B cells, which express NP-specific BCR (Fig. 3A). In a previous report, we showed that CD45⁻ICAM-1⁺ cells supported the survival naïve B cells (Usui et al., 2012).

Consistent with this previous report, in the present study CD45$^-$ICAM-1$^+$ cells significantly enhanced B-cell survival and proliferation compared with negative control ($P < 0.001$; Fig. 3B–E). Furthermore, compared with CD45$^-$ICAM-1$^+$ cells, CD45$^-$ICAM-1$^+$CD21/35$^+$ cells significantly prolonged QM B-cell survival ($P < 0.001$; Fig. 3B, C) and dramatically induced the proliferation of QM B cells ($P < 0.001$; Fig. 3D, E). To examine whether CD45$^-$ICAM-1$^+$CD21/35$^+$ cells stimulate B cell proliferation in an antigen-dependent manner, CD45$^-$ICAM-1$^+$CD21/35$^+$ cells from mice administered NP-Ficoll were co-cultured with CFSE-labeled B cells derived from WT mice. In contrast to QM B cells, WT B cells showed little proliferation (Fig. 3 F, G), demonstrating that CD45$^-$ICAM-1$^+$CD21/35$^+$ cells stimulated B cell proliferation in an antigen-dependent manner. Taken together, CD45$^-$ICAM-1$^+$CD21/35$^+$ cells maintained their antigen-presentation abilities even after isolation via flow cytometry, suggesting that these cells are useful for the functional analysis of FDCs *in vitro*.

In conclusion, $CD45^{-}ICAM\text{-}1^{+}CD21/35^{+}$ cells obtained with our improved protocol showed the following features typical of FDCs: 1) they were rare (0.07 % in stromal cell-enriched fractions of naïve spleen), 2) they had a comparable phenotype (FDC marker expression), and 3) they had comparable functions (antigen retention *in vivo* and antigen presentation to cognate B cells). Together, these data indicate that we were able to define $CD45^{-}ICAM\text{-}1^{+}CD21/35^{+}$ cells phenotypically and functionally as a highly enriched FDC population. Our improved protocol therefore allows the isolation of a highly enriched preparation of viable FDCs without the need for treatments such as irradiation or immunization, which means that these cells are suitable for use in biochemical and genetic analyses of naïve FDCs.

1 Acknowledgments

2 We thank S. Tochihara and Y. Nomura for their secretarial assistance. This
3 study was supported in part by grants provided by the Ministry of Education,
4 Culture, Sports, Science and Technology of Japan (Grant number 16H06387
5 to AS and Grant number 16H05169 to K. Shibuya) and a grants-in-aid
6 provided by the Japan Society for the Promotion of Science Fellows (Grant
7 number 14J00713 to K. Sato).

8

9

4. References

Allen, C.D.C., Cyster, J.G., 2008. Follicular dendritic cell networks of primary follicles and germinal centers: Phenotype and function. Semin. Immunol. 20, 14–25. doi:10.1016/j.smim.2007.12.001

Castagnaro, L., Lenti, E., Maruzzelli, S., Spinardi, L., Migliori, E., Farinello, D., Sitia, G., Harrelson, Z., Evans, S.M., Guidotti, L.G., Harvey, R.P., Brendolan, A., 2013. Nkx2-5+Islet1+ Mesenchymal Precursors Generate Distinct Spleen Stromal Cell Subsets and Participate in Restoring Stromal Network Integrity. Immunity 38, 782–791. doi:10.1016/j.immuni.2012.12.005

Chen, L.L., Adams, J.C., Steinman, R.M., 1978a. Anatomy of germinal centers in mouse spleen, with special reference to "follicular dendritic cells". J. Cell Biol. 77, 148–64.

Chen, L.L., Frank, A.M., Adams, J.C., Steinman, R.M., 1978b. Distribution of horseradish peroxidase (HRP)-anti-HRP immune complexes in mouse

spleen with special reference to follicular dendritic cells. J. Cell Biol. 79, 184–99. doi:10.1083/jcb.79.1.184

Fasnacht, N., Huang, H.-Y., Koch, U., Favre, S., Auderset, F., Chai, Q., Onder, L., Kallert, S., Pinschewer, D.D., MacDonald, H.R., Tacchini-Cottier, F., Ludewig, B., Luther, S. a., Radtke, F., 2014. Specific fibroblastic niches in secondary lymphoid organs orchestrate distinct Notch-regulated immune responses. J. Exp. Med. doi:10.1084/jem.20132528

Heesters, B.A., Chatterjee, P., Kim, Y.-A., Gonzalez, S.F., Kuligowski, M.P., Kirchhausen, T., Carroll, M.C., 2013. Endocytosis and Recycling of Immune Complexes by Follicular Dendritic Cells Enhances B Cell Antigen Binding and Activation. Immunity 38, 1164–1175. doi:10.1016/j.immuni.2013.02.023

Honda, S., Kurita, N., Miyamoto, A., Cho, Y., Usui, K., Takeshita, K., Takahashi, S., Yasui, T., Kikutani, H., Kinoshita, T., Fujita, T., Tahara-Hanaoka, S., Shibuya, K., Shibuya, A., 2009. Enhanced humoral

immune responses against T-independent antigens in Fc / R-deficient mice. Proc. Natl. Acad. Sci. 106, 11230–11235. doi:10.1073/pnas.0809917106

Jarjour, M., Jorquera, A., Mondor, I., Wienert, S., Narang, P., Coles, M.C., Klauschen, F., Bajénoff, M., 2014. Fate mapping reveals origin and dynamics of lymph node follicular dendritic cells. J. Exp. Med. 211, 1109–1122. doi:10.1084/jem.20132409

Kranich, J., Krautler, N.J., Heinen, E., Polymenidou, M., Bridel, C., Schildknecht, A., Huber, C., Kosco-Vilbois, M.H., Zinkernagel, R., Miele, G., Aguzzi, A., 2008. Follicular dendritic cells control engulfment of apoptotic bodies by secreting Mfge8. J. Exp. Med. 205, 1293–1302. doi:10.1084/jem.20071019

Krautler, N.J., Kana, V., Kranich, J., Tian, Y., Perera, D., Lemm, D., Schwarz, P., Armulik, A., Browning, J.L., Tallquist, M., Buch, T., Oliveira-Martins, J.B., Zhu, C., Hermann, M., Wagner, U., Brink, R., Heikenwalder, M., Aguzzi, A., 2012. Follicular Dendritic Cells Emerge

from Ubiquitous Perivascular Precursors. Cell 150, 194–206. doi:10.1016/j.cell.2012.05.032

Link, A., Vogt, T.K., Favre, S., Britschgi, M.R., Acha-Orbea, H., Hinz, B., Cyster, J.G., Luther, S.A., 2007. Fibroblastic reticular cells in lymph nodes regulate the homeostasis of naive T cells. Nat. Immunol. 8, 1255–1265. doi:10.1038/ni1513

Mandel, T.E., Phipps, R.P., Abbot, A., Tew, J.G., 1980. The follicular dendritic cell: long term antigen retention during immunity. Immunol. Rev. 53, 29–59. doi:10.1111/j.1600-065X.1980.tb01039.x

Mitchell, J., Abbot, A., 1965. Ultrastructure of the Antigen-retaining Reticulum of Lymph Node Follicles as shown by High-resolution Autoradiography. Nature 208, 500–502. doi:10.1038/208500b0

Schaue, D., Micewicz, E.D., Ratikan, J.A., Xie, M.W., Cheng, G., McBride, W.H., 2015. Radiation and inflammation. Semin. Radiat. Oncol. 25, 4–10. doi:10.1016/j.semradonc.2014.07.007

Sørensen, K.K., McCourt, P., Berg, T., Crossley, C., Le Couteur, D., Wake, K.,

Smedsrød, B., 2012. The scavenger endothelial cell: a new player in homeostasis and immunity. Am. J. Physiol. Regul. Integr. Comp. Physiol. 303, R1217–30. doi:10.1152/ajpregu.00686.2011

Sukumar, S., Szakal, A.K., Tew, J.G., 2006. Isolation of functionally active murine follicular dendritic cells. J. Immunol. Methods 313, 81–95. doi:10.1016/j.jim.2006.03.018

Tamburini, B.A., Burchill, M.A., Kedl, R.M., 2014. Antigen capture and archiving by lymphatic endothelial cells following vaccination or viral infection. Nat. Commun. 5. doi:10.1038/ncomms4989

Turley, S.J., Fletcher, A.L., Elpek, K.G., 2010. The stromal and haematopoietic antigen-presenting cells that reside in secondary lymphoid organs. Nat. Rev. Immunol. 10, 813–25. doi:10.1038/nri2886

Usui, K., Honda, S., Yoshizawa, Y., Nakahashi-Oda, C., Tahara-Hanaoka, S., Shibuya, K., Shibuya, A., 2012. Isolation and characterization of naïve follicular dendritic cells. Mol. Immunol. 50, 172–176. doi:10.1016/j.molimm.2011.11.010

Victora, G.D., Nussenzweig, M.C., 2012. Germinal centers. Annu. Rev. Immunol. 30, 429–57. doi:10.1146/annurev-immunol-020711-075032

Table 1. Average number and percentage of cells in stromal cell subsets isolated from a single naïve mouse spleen.

Percentages were calculated from the number of PI^- gated cells from stromal cell-enriched fractions of naive mouse spleen after negative selection via biotinylated anti CD45, B220 and Ter119 followed by streptavidin magnetic beads. Data are representative of four experiments with three mice per replicate.

Fig. 1. Isolation and characterization of naïve CD45$^-$ICAM-1$^+$CD21/35$^+$ cells.

(A) Sorting strategy for the isolation of blood endothelial cells (BECs, CD45$^-$ICAM-1$^+$CD31$^+$), fibroblastic reticular cells (FRCs, CD45$^-$ICAM-1$^+$PDPN$^+$), CD45$^-$ICAM-1$^+$CD21/35$^+$ cells, and CD45$^-$ICAM-1$^+$ cells from a stromal cell-enriched fraction from the spleen of naive mice. Numbers indicate the percentage of cells in each population. Representative plots of staining of B220 (B) and FDC-M2 (C). Open and shaded histograms indicate staining with indicated mAb and isotype control, respectively. Numbers indicate the mean fluorescence intensity (MFI). (D, E) The mRNA expression levels of FDC markers (B) and other stromal cell subset markers (C) were determined relative to those in CD45$^-$ICAM-1$^+$ cells. Statistical significance is shown compared with CD45$^-$ICAM-1$^+$ cells. (D, E) Data were pooled from three independent experiments. Error bars indicate SD. ***$P < 0.001$

Fig. 2. Antigen retention by CD45$^-$ICAM-1$^+$CD21/35$^+$ cells isolated from antigen-administered mice

Flow cytometric analysis of antigen retention by stromal cells isolated from mice intravenously administered 50 μg FITC-labeled TNP-Ficoll or phosphate-buffered saline (PBS) on day 7 after antigen administration. (A) Representative histograms (open histogram: antigen [Ag]-injected mice; shaded histogram, phosphate-buffered saline [PBS] control mice) showing retention of FITC-conjugated antigen by CD45$^-$ICAM-1$^+$ cells, blood endothelial cells (BECs, CD45$^-$ICAM-1$^+$CD31$^+$), fibroblastic reticular cells (FRCs, CD45$^-$ICAM-1$^+$PDPN$^+$), and CD45$^-$ICAM-1$^+$CD21/35$^+$ cells. (B) Quantification data showing the mean fluorescence intensity (MFI) of each stromal cell subset isolated from the injected mice (n = 3) divided by that of PBS-administered control mice (n = 3). Data are pooled from three independent experiments. Error bars indicate SD. $^{**}P < 0.01$.

Fig. 3. Antigen presentation to cognate B cells by isolated $CD45^{-}ICAM\text{-}1^{+}CD21/35^{+}$ cells

Schematic representation of the experimental protocol: CFSE-labeled naive QM B cells (B-G) and WT B cells (F, G) were co-cultured for 3 days in 96-well round-bottom plates with either $CD45^{-}ICAM\text{-}1^{+}$ cells or $CD45^{-}ICAM\text{-}1^{+}CD21/35^{+}$ cells isolated from mice given 50 μg NP-Ficoll intravenously seven days previously. Cells were harvested and stained with anti-CD19 monoclonal antibodies, and $CD19^{+}$ cells and $CD19^{+}PI^{-}$ cells were examined by means of flow cytometry for survival (B, C) and proliferation (D-G), respectively. (B) Representative plots showing $CD19^{+}$-gated cells. PI^{-} cells were considered live B cells. (C) Bar graph showing the percentage of PI^{-} cells in $CD19^{+}$ gated (n = 3). (D-G) B-cell proliferation was analyzed by means of a CFSE-dilution assay. (D, F) Representative histograms showing $CD19^{+}PI^{-}$-gated cells co-cultured or not with $CD45^{-}ICAM\text{-}1^{+}$ cells or $CD45^{-}ICAM\text{-}1^{+}CD21/35^{+}$ cells. Numbers represent the frequency of divided B cells. (E, G) Bar graph indicating the percentage of divided B cells in the

1 $CD19^{+}PI^{-}$-gated (n = 3). (B-G) Data are pooled from at least two independent

2 experiments. Error bars indicate SD. ***$P < 0.001$. n.s., not significant.

3

Supplementary Fig. 1 CD21/35 expression after collagenase D treatment.

Spleen cells were treated with high (33.3 mg/ml) or low (1mg/ml) concentration of collagenase D for 30 min at 37 ℃ and stained with anti-CD45 mAb. Representative plots of CD21/35 staining in $CD45^+$ gated cells. Open and shaded histograms indicate staining with anti-CD21/35 mAb and isotype control, respectively.

Table 1.

	Dispase	Cell number		Percentage	
		Mean	SD	Mean	SD
$CD45^{-}ICAM\text{-}1^{+}$ cells	+	276.88	26.0	61.00	4.65
$CD45^{-}ICAM\text{-}1^{+}CD31^{+}$ cells (BECs)	+	269.96	25.7	59.47	4.48
$CD45^{-}ICAM\text{-}1^{+}PDPN^{+}$ cells (FRCs)	+	1.77	0.4	0.39	0.06
$CD45^{-}ICAM\text{-}1^{+}CD21/35^{+}$ cells	+	0.34	0.1	0.07	0.03
$CD45^{-}ICAM\text{-}1^{+}CD21/35^{+}$ cells	–	0.12	0.04	0.07	0.02
		(x 10e3 cells)		(% of Live cells)	

Figure 1

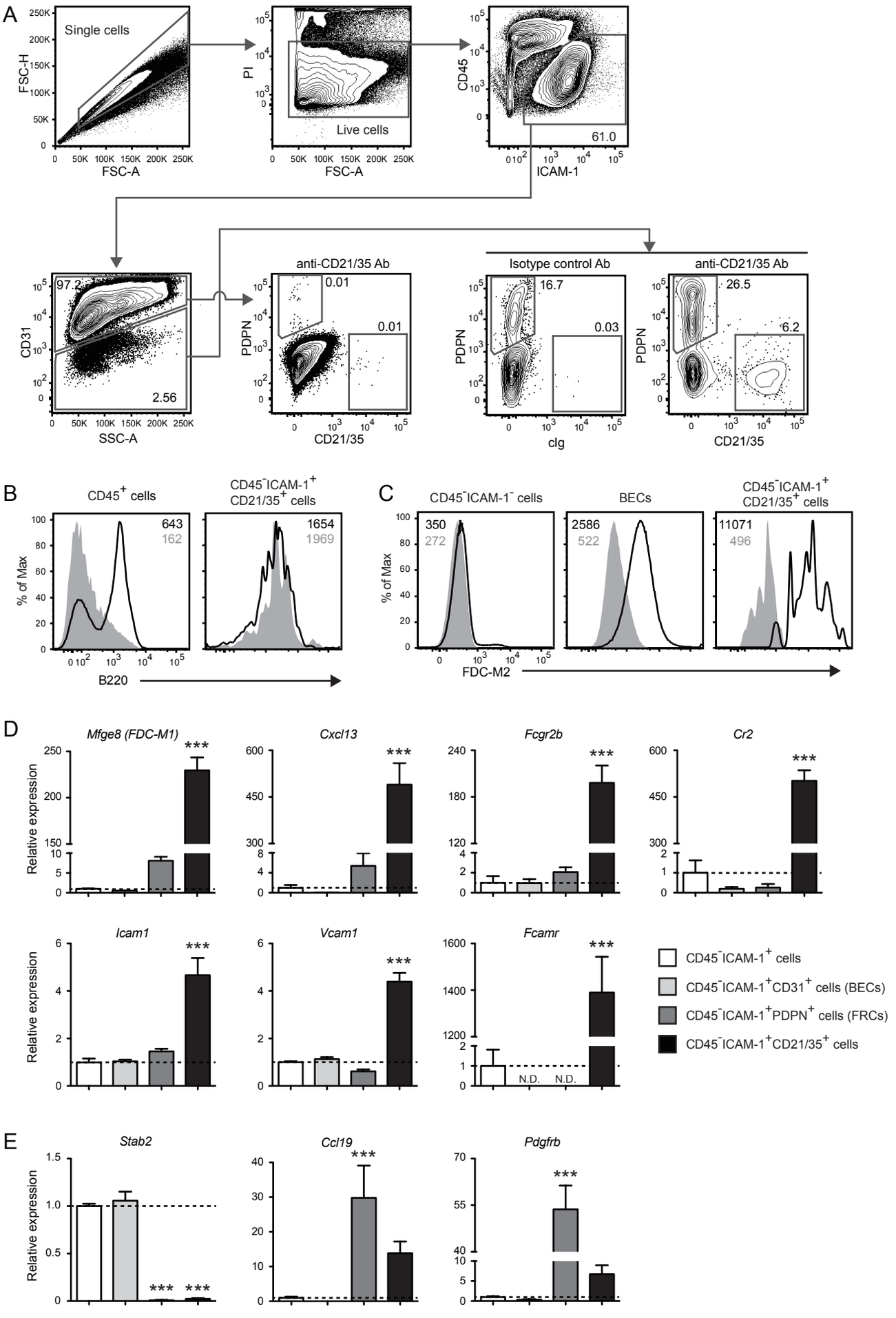
A
Single cells
FSC-H
FSC-A
PI
Live cells
CD45
61.0
ICAM-1
97.2
CD31
2.56
SSC-A
anti-CD21/35 Ab
0.01
0.01
PDPN
CD21/35
Isotype control Ab
16.7
0.03
clg
anti-CD21/35 Ab
26.5
6.2
B
CD45+ cells
CD45-ICAM-1+ CD21/35+ cells
643
162
1654
1969
% of Max
B220
C
CD45-ICAM-1- cells
BECs
CD45-ICAM-1+ CD21/35+ cells
350
272
2586
522
11071
496
FDC-M2
D
Mfge8 (FDC-M1)
Cxcl13
Fcgr2b
Cr2
Icam1
Vcam1
Fcamr
Relative expression
N.D.
CD45-ICAM-1+ cells
CD45-ICAM-1+CD31+ cells (BECs)
CD45-ICAM-1+PDPN+ cells (FRCs)
CD45-ICAM-1+CD21/35+ cells
E
Stab2
Ccl19
Pdgfrb
Relative expression

Figure 2

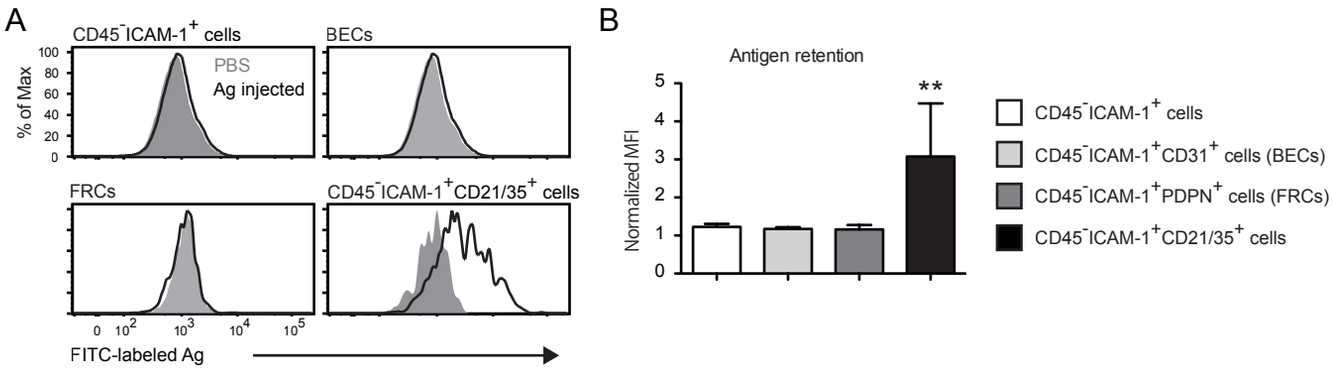
A
CD45-ICAM-1+ cells
BECs
PBS
Ag injected
% of Max
100
80
60
40
20
0
FRCs
CD45-ICAM-1+CD21/35+ cells
0
10^2
10^3
10^4
10^5
FITC-labeled Ag
B
Antigen retention
Normalized MFI
5
4
3
2
1
0
**
CD45-ICAM-1+ cells
CD45-ICAM-1+CD31+ cells (BECs)
CD45-ICAM-1+PDPN+ cells (FRCs)
CD45-ICAM-1+CD21/35+ cells

Figure 3

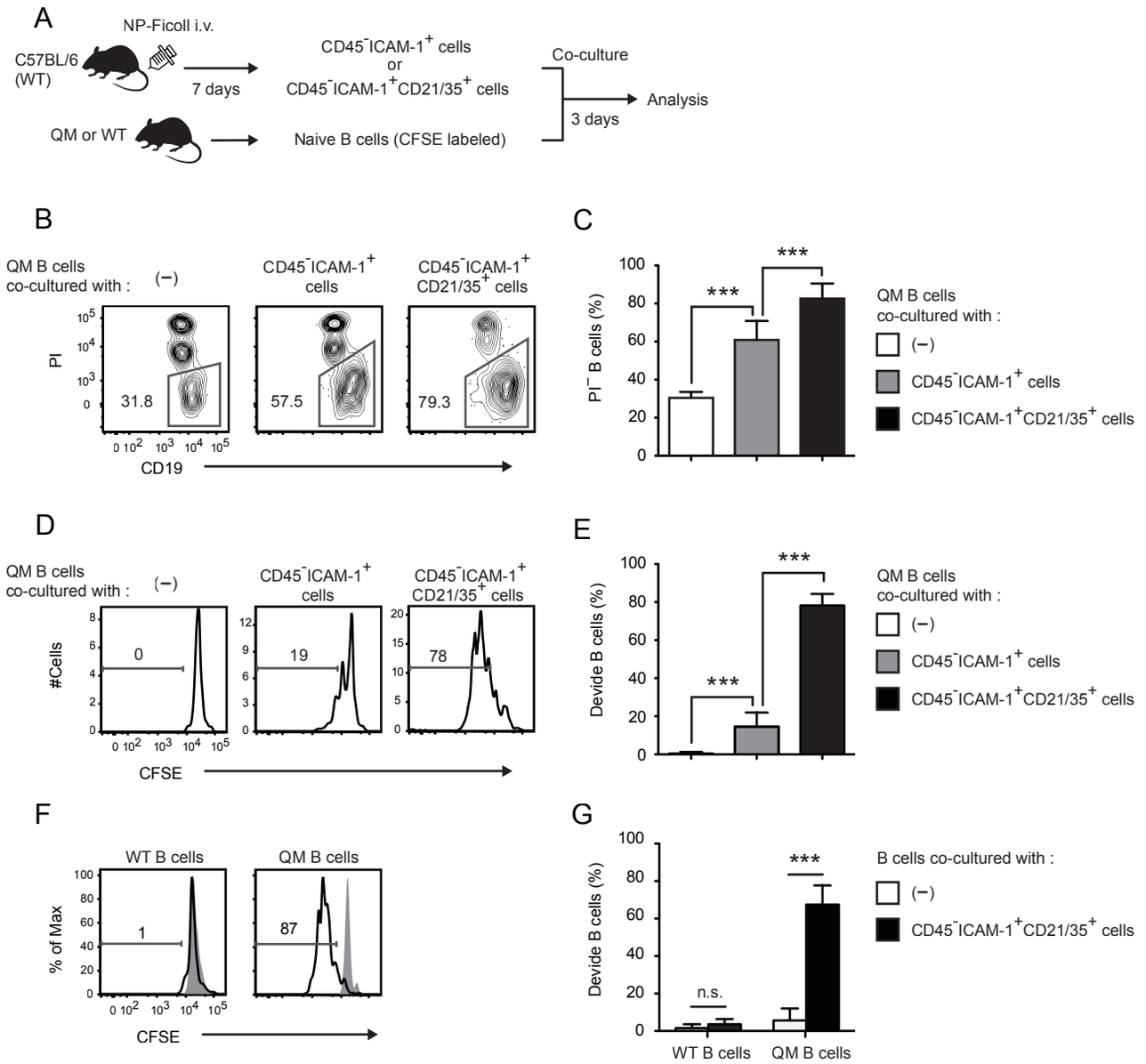
A
NP-Ficoll i.v.
C57BL/6 (WT)
7 days
CD45-ICAM-1+ cells or CD45-ICAM-1+CD21/35+ cells
QM or WT
Naive B cells (CFSE labeled)
Co-culture
3 days
Analysis
B
QM B cells co-cultured with :
(−)
CD45-ICAM-1+ cells
CD45-ICAM-1+ CD21/35+ cells
PI
CD19
31.8
57.5
79.3
C
PI− B cells (%)
***
QM B cells co-cultured with :
(−)
CD45-ICAM-1+ cells
CD45-ICAM-1+CD21/35+ cells
D
#Cells
CFSE
0
19
78
E
Devide B cells (%)
***
F
WT B cells
QM B cells
% of Max
1
87
CFSE
G
Devide B cells (%)
n.s.
***
WT B cells
QM B cells
B cells co-cultured with :
(−)
CD45-ICAM-1+CD21/35+ cells

Supplementary Figure 1